TiO_2 SURFACES MODIFICATION FOR AMOXICILLIN RELEASE USED IN DENTAL IMPLANTOLOGY

Angela Gabriela PĂUN[1]

The present research is focused on the possibility of amoxicillin entrapment on the TiO_2 nanostructured surface on Titanium film. For this purpose, nanostructures obtained in different anodizing conditions were synthesized. The samples were characterized in terms of morphology, wettability, electrochemical stability. The ability to release the antibiotic was investigated to highlight the differences between the nanostructures. According to the data obtained, these substrates are excellent candidates for amoxicillin binding.

The new surfaces coated with reduced TiO_2 nanotubes may be used as an interlayer for the antibiotic's incorporation and local release for dental implantable surfaces.

Keywords: TiO_2 nanotubes, "reduced" TiO_2 nanotubes, amoxicillin.

1. Introduction

A wide range of chemical, physical, biological, and mechanical stimulations can affect the dynamic properties of the oral cavity. A variety of dental disorders (tooth loss, periodontal disease, trauma, etc.) are brought on by bacteria growth and biofilm formation in the hard and soft tissues of the mouth cavity. Finding a material type that can treat various oral disorders is therefore necessary [1-6].

Titanium (Ti) and titanium-based alloys are the most widely used metallic materials in dental and orthopedic implantology, because they present high biocompatibility, corrosion resistance, flexibility and mechanical resistance [7-10]. Comparing to stainless steel, chromium, and cobalt-nickel alloys, they are more biocompatible, because of their low elastic modulus and low ion release when exposed to body fluids [11]. Because of its poor electrical conductivity, titanium is able to produce an atmospheric passivation oxide layer that is chemically stable, giving the metal its excellent biocompatibility. It prevents surface corrosion, and it is responsible for its high surface energy characteristics [7, 11-13]. However, Ti has no intrinsic antibacterial properties, causing low osseointegration. Thus, infections may happen at the implant level, conducting to failure and prolonged hospitalization [9, 10, 14]. In these situations, surface modification is crucial to promote osteogenesis and creating the right interfacial microenvironments at the implant-bone tissue interface [8, 10]. Titanium and its alloys can be modified with

[1] Dept. of General Chemistry, University POLITEHNICA of Bucharest, Romania, e-mail: angela.olaru@upb.ro

titanium dioxide nanotubes (NT) that have the ability to improve contact between the implant surface and the bone. Surfaces modified with NT have the ability to enhance osseointegration. The manufactured surfaces have better mechanical and chemical properties and the advantage of loading drugs/active agents for local delivery [7, 10, 15]. These nanotubular structures directly influence interactions with cells. Biocompatibility of NT or the ability to differentiate particular cell types can both be facilitated by the incorporation of particular growth factors [16-18].

Recently, "reduced" TiO_2 nanostructures have attracted much attention recently. They are obtained through reduction treatments, which induce the formation of Ti^{3+} and free oxygen sites in the walls of the nanotubes. Reduced TiO_2 nanostructures (RnT) have better properties for biomedical applications, water splitting and photocatalysis compared to non-reduced TiO_2. One of the advantages is the reduction of the bandgap (< 3 eV), which causes an increased surface conductivity and a decrease in the electron transport time [16, 19, 20]. The advantage of these new implants is their use as electrodes for electrical stimulation therapy with simultaneous local drug release, increased intracellular calcium and osteogenic differentiation of mesenchymal stem cells [16, 21, 22].

This paper describes the NT and RnT nanostructured surfaces preparation, nanostructures designed for loading and controlled release of various therapeutic compounds. On these nanostructures amoxicillin for controlled release was embedded. The samples were evaluated morphologically and electrochemically and the ability to incorporate and release the drug was evaluated by UV analysis.

2. Experimental section

*2.1 **Materials***

In this study, titanium foils were used as support material. The Ti samples were polished using abrasive sheets of different porosities and cleaned in distilled water, ethanol and acetone for 15 min by ultrasounds.

Other reagents used in this study were: Sodium phosphate dibasic dihydrate ($Na_2HPO_4 \cdot 2H_2O$), sodium phosphate monobasic dihydrate ($NaH_2PO_4 \cdot 2H_2O$), Ethylene glycol – anhydrous (99.8% purity) (EG), Ammonium fluoride. All reagents were provided by Sigma Aldrich.

*2.2 **Preparation of TiO_2 nanotube structures***

TiO_2 nanotube structures were prepared through an anodization process which was effectuated in an electrochemical cell using two electrodes, a Ti electrode (anode) and a Pt electrode (cathode). The anodizing was performed in different electrolytes, using a MATRIX MPS-7163 source, and applying the voltage specified in Table 1 [23, 24].

Table 1

Composition of the anodizing electrolyte solutions and the voltage utilized

Sample	Electrolyte composition	Voltage applied (V)	Time h	Sample name
Titanium	NH_4F (0.5% wt) + distilled water (2% v) + EG	40	3	NT_40V
	NH_4F (0.2% wt) + H_2O_2 (10% v) + EG	80	2	NT_80V

After anodizing the samples obtained were rinsed with distilled water and then calcined for 2 hours at 450°C. Following calcination, NT_40V and NT_80V samples were activated at 4V for 600s in an anodization solution. Subsequently, the samples were reduced at -40V in organic solution containing NH_4F (0.25% wt) and EG. These samples were named RnT_40V and RnT_80V [25].

*2.3 **Amoxicillin embedding***

All modified samples were submerged in 10 mL of aqueous amoxicillin solution (3g/L) for 48 hours, at room temperature. The samples were then washed with distilled water to eliminate any unabsorbed antibiotic. Amoxicillin loaded samples were named **Ti/AMX, NT_40V/AMX, NT_80V/AMX, RnT_40V/AMX and RnT_80V/AMX**.

*2.4 **Samples characterization***

SEM analysis was used for the morphological characterization of the sample surfaces. This was accomplished using SEM equipment, model FEI/Philips XL-30 QUANTA 650.

FTIR analysis was used to obtain the infrared spectra. This method was carried out utilizing an FTIR equipment, Spectrum 100 (PerkinElmer USA). All of the readings were taken between 1000 and 4000 cm^{-1}.

Surface wettability was appreciated using the Sessile Drop method by CAM 100 Optical Contact Angle Meter. Different areas on the coated surface were used to measure the contact angle's value.

The electrochemical tests of the modified samples were performed in a cell with three electrodes using an Autolab 302N with a Nova 1.10 software. All samples were examined in 0.9% sodium chloride solution (NaCl), at room temperature.

Tafel diagrams were recorded between -260 mV and +150 mV compared to the OCP (open circuit potential), at a scanning rate of 2 mV / s. At the same time, Electrochemical impedance spectra (EIS) were registered in the frequency range of 0.1 - 10^5Hz with an amplitude of 10 mV. Cyclic voltammetry curves (CV) were recorded in the range (-1.5V; 1V), with a scanning rate of 50 mV / s.

*2.5 **Amoxicillin release studies***

For release studies, all modified samples were immersed in amoxicillin solution at 3 g/L concentration for 48 hours. The samples were then submerged into a 10 mL phosphate buffer (PBS) having a neutral pH of 7.4. The drug concentration released over time in the PBS was determined by UV-VIS spectroscopy at 232 nm wavelength (λ).

The amount of amoxicillin released was determined using a calibration curve with a linear regression equation: y = 0.008x+0.00086 and a correlation coefficient (R2) of 0.999 in the concentration range of 4-60 mg/L amoxicillin.

3. Results and discussion

*3.1 **Surfaces morphology***

Figure 1 shows SEM images of titanium dioxide nanotubes obtained by electrochemical anodization with and without amoxicillin (NT_40V, NT_80V, RnT_40V RnT_80V, NT_40V/AMX, NT_80V/AMX, RnT_40V/AMX and RnT_80V/AMX). The surface of Ti samples is covered entirely with self-organized nanotubes that have different heights but uniform diameters. It can be seen that AMX does not influence the morphology of the nanotubes. The presence of amoxicillin on the nanotubes surface is not visible considering that a small amount of this compound was attached.

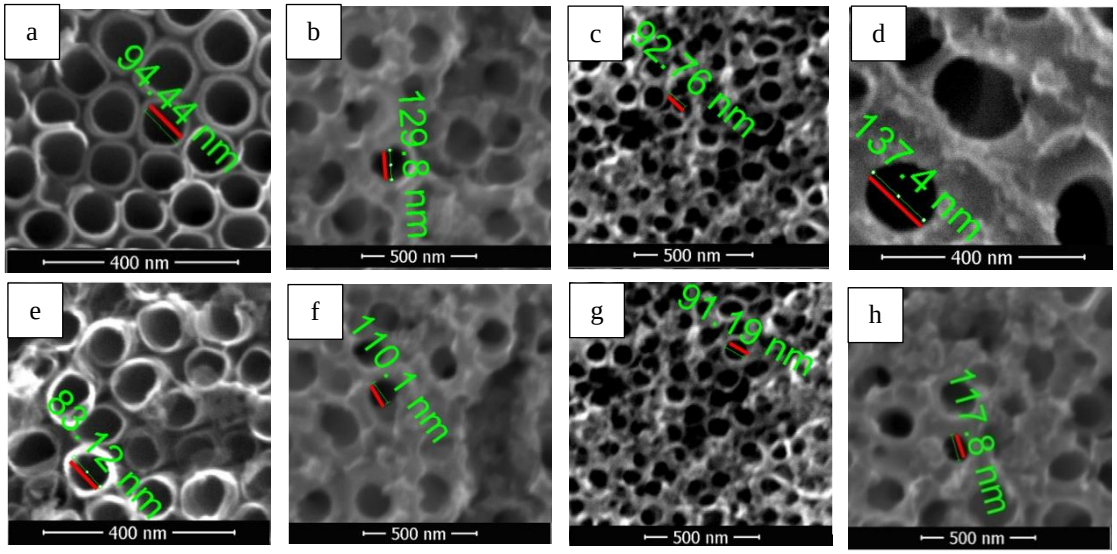

Fig. 1. SEM images corresponding to the nanostructured samples: a) NT_40V; b) NT_80V; c) RnT_40V; d) RnT_80V; e) NT_40V/AMX; f) NT_80V/AMX; g) RnT_40V/AMX; h) RnT_80V/AMX

For each sample, 20 nanotube diameters were measured using the ImageJ program. Then, the mean value and standard deviation for all sample diameters were calculated using Excel. As shown in Table 2, the average diameters are between 92.50 nm and 128.88 nm, respectively the standard deviation values being between 2.62 and 7.61 Considering these low values for standard deviations, it is obviously that all samples have uniform surfaces.

Table 2

Average diameters and standard deviation of modified surfaces

Samples	Average diameter	Standard deviation
NT_40V	92.50	6.88
NT_40V/AMX	90.03	5.61
NT_80V	122.05	7.61
NT_80V/AMX	112.93	6.86
RnT_40V	94.70	7.52
RnT_40V/AMX	89.38	4.85
RnT_80V	128.88	6.30
RnT_80V/AMX	118.33	2.62

*3.2 **FT-IR analysis***

As shown in Fig. 2, the N-H stretching, O-H stretching, C=O carboxyl, C=O amide, N-H bending, C=C, O-H bending, C-N bending and C-O groups can be identified in the infrared absorption spectra of amoxicillin powder at 3449, 3162, 1780, 1687, 1574, 1487, 1398, 1315, and 1252 cm^{-1} [26]. Nanostructured samples modified with amoxicillin (NT_40V/AMX, NT_80V/AMX, RnT_40V/AMX and RnT_80V/AMX) show the same peaks. This indicate that AMX was loaded on the nanostructured surfaces.

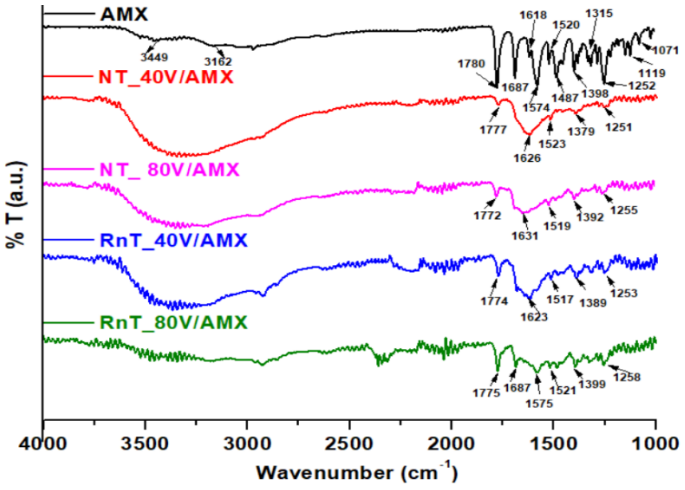

Fig. 2. FT-IR spectra of nanostructured samples incorporating amoxicillin

*3.3 **Surface wettability***

The contact angles values for water drops deposited on the nanostructured surfaces are presented in Table 3. All modified samples with amoxicillin have a contact angle value between 17° to 21°, being largely in agreement with the findings of other investigations [27]. There is not a visible difference in the wettability of these samples, all of them possessing a powerful hydrophilic character. This might be advantageous for improved cell attachment and proliferation on the surface of implantable materials [28].

Table 3

The contact angle of modified surfaces

Samples	Contact angle θ (◦)	Standard deviation θ (◦)
NT_40V/AMX	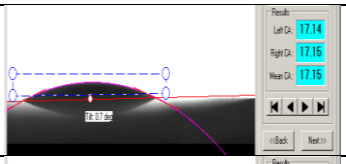	0.52
NT_80V/AMX	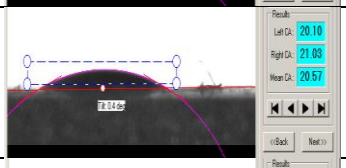	0.42
RnT_40V/AMX	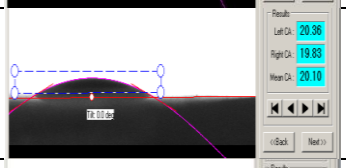	0.45
RnT_80V/AMX	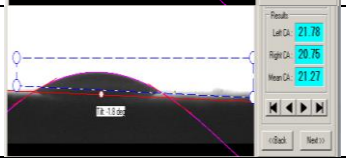	0.48

Three successive measurements were taken for each of the four samples, and the mean value was recorded into Excel. For each sample, we determined the average and the standard deviation for water contact angle (shown in table 3). The standard deviation values were: 0.52 for NT_40V/AMX, 0.42 for NT_80V/AMX, 0.45 for RnT_40V/AMX, and 0.48 for RnT_80V/AMX. The low standard deviation results suggest that the sample surface is uniform.

3.4 Electrochemical characterization

3.4.1 Tafel analysis

In order to perform electrochemical studies, Ti modified samples were characterized in terms of corrosion. The Tafel plot enables the determination of the corrosion potential (E_{corr}), corrosion current density (i_{corr}), and corrosion rate (v_{corr}) of the investigated surfaces. Fig. 3 shows the Tafel plots of the modified samples surface. Ti/AMX has the lowest corrosion current and higher electropositive potential compared to the other samples, thus it is less susceptible to corrosion.

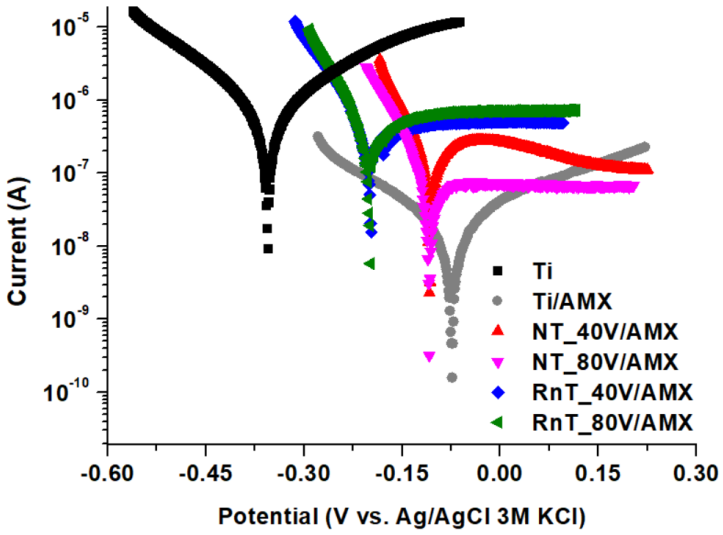

Fig. 3. Tafel diagram for the Ti modified samples

The corrosion parameters were calculated using NOVA software by extrapolating the both cathodic and anodic curves (Table 4).

Table 4

The principal corrosion parameters

Samples	Corrosion potential (V)	Corrosion current density (A/cm^2)	Corrosion rate (mm/year)
Ti	-0.35	$9.58 \cdot 10^{-7}$	$111 \cdot 10^{-4}$
Ti/AMX	-0.08	$2.5 \cdot 10^{-7}$	$18.32 \cdot 10^{-4}$
NT_40V/AMX	-0.10	$4.58 \cdot 10^{-7}$	$53.28 \cdot 10^{-4}$
NT_80V/AMX	-0.11	$3.26 \cdot 10^{-7}$	$37.873 \cdot 10^{-4}$
RnT_40V/AMX	-0.20	$6.47 \cdot 10^{-7}$	$75.22 \cdot 10^{-4}$
RnT_80V/AMX	-0.20	$7.16 \cdot 10^{-7}$	$84.805 \cdot 10^{-4}$

The Ti/AMX sample is the most stable in terms of corrosion, having the lowest corrosion rate when compared to the other samples. According to our investigations, AMX represents a protective layer for the Ti surface, reducing the corrosion rate for Ti/AMX compared to the Ti sample [27]. The corrosion rate and

corrosion current densities increased slightly when AMX was loaded into the nanotubes substrate, most likely because of the interaction between AMX and these nanostructures. However, as compared to titanium substrate, the corrosion rate is significantly reduced for all modified samples.

3.4.2 Impedance diagrams

Electrochemical impedance spectroscopy (EIS) was used to highlight the processes occurring at the electrolyte-biomaterial interface, such as charge transport characteristics. Fig. 4 shows the Nyquist plots correlating with the analysed samples. As a first observation, from EIS analysis: all modified samples have higher resistance than untreated Ti, being more stable.

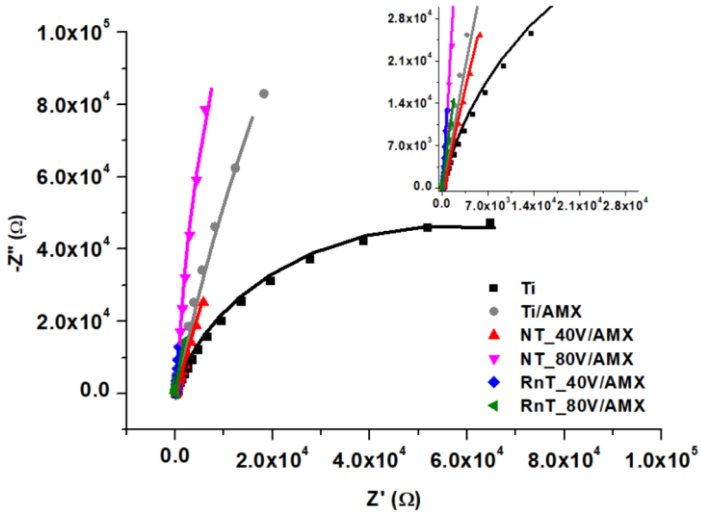

Fig. 4. Nyquist diagrams of modified samples, performed in NaCl (aq).

Fig. 5 presents the equivalent circuits that helped fitting all data. The first circuit (Fig. 5 a) was used for titanium substrate. It mainly consists of the biofluid's resistance ($R_{solution}$), in series with a circuit formed of a resistance (R_{oxide}), in parallel with a constant phase element (CPE_{oxide}) that corresponds to the native barrier oxide layer.

For all Ti modified samples it was used the circuit showed in Fig. 5 b. This circuit is composed from the resistance of the solution ($R_{solution}$), specific circuit corresponding to the oxide layer and specific circuit corresponding to the coated substrate.

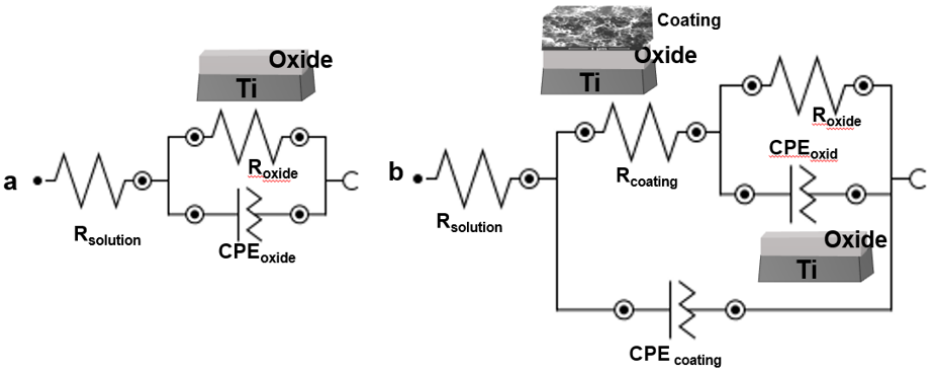

Fig. 5. Equivalent circuits used to fit EIS data for: a. Titanium substrate; b. modified samples

The circuit parameters, obtained using the Nova software, are presented in Table 5. Taking into account the similarity of the electrolyte and test conditions, the solution resistance is practically identical for all examined samples (approximately 100 Ω). It can be seen that following surface coating, the R_{oxid} increases when compared to titanium substrate. The resistance of the nanotubular layers is higher compared with Ti sample. The deposition of amoxicillin does not bring significant changes in resistance. The native oxide layer's N values for all samples are around 0.9, which suggests a pseudocapacitive behaviour. For the coating layer, N values are smaller than 0.5 indicating pseudo-resistive behaviour.

Table 5

Parameters obtained by equivalent circuits

Parameter/ Sample	R_S (Ω)	$R_{coating}$ (Ω)	$CPE_{coating}$		R_{oxide} (Ω)	CPE_{oxide}		X^2
			Y_0 ($S*s^n$)	N		Y_0 ($S*s^n$)	N	
Ti	75.5	-	-	-	$0.11\cdot10^6$	$2.60\cdot10^{-5}$	0.87	0.07
Ti/AMX	97.8	$2.0\cdot10^2$	$0.80\cdot10^{-3}$	0.43	$1.10\cdot10^6$	$1.83\cdot10^{-5}$	0.91	0.06
NT_40V/AMX	99	$7.0*10^2$	$2.31\cdot10^{-3}$	0,45	$0.87\cdot10^6$	$19.31\cdot10^{-5}$	0.89	0.23
NT_80V/AMX	89	$9.0*10^2$	$1.45\cdot10^{-3}$	0.47	$1.11\cdot10^6$	$18.64\cdot10^{-5}$	0.99	0.21
RnT_40V/AMX	96.8	$9.1*10^2$	$31.40\cdot10^{-3}$	0.39	$2.00\cdot10^6$	$0.11\cdot10^{-5}$	0.97	0.01
RnT_80V/AMX	74.5	$9.0*10^2$	$11.01\cdot10^{-3}$	0.47	$0.62\cdot10^6$	$9.12\cdot10^{-5}$	0.94	0.01

3.4.3 Cyclic voltammetry

Using the CV diagrams (Fig. 6), the double-layer capacitance (C_{dl}) for the studied samples was calculated and the results are presented in table 6. The equation for C_{dl} is as follows [19]:

$$C_{dl} = \frac{i}{\vartheta} \quad (1)$$

where "i" is average current density recorded during the potential sweep from 0 V to 1 V in anodic direction and "ϑ" is scan rate.

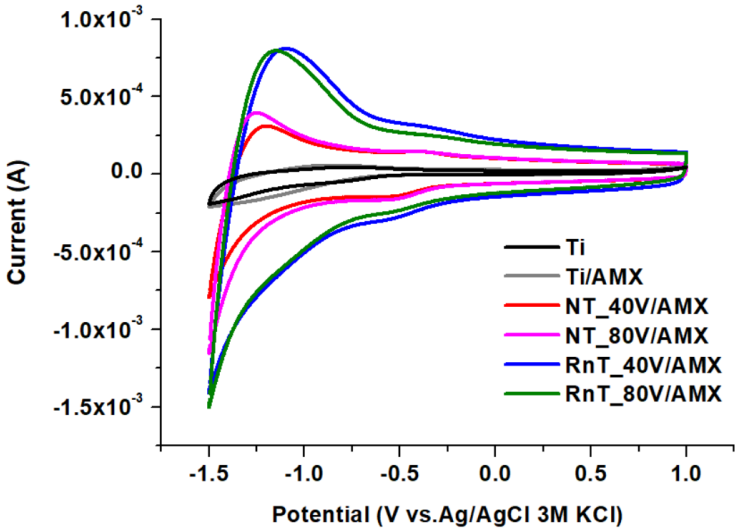

Fig. 6. Cyclic voltammetry for all modified samples

It can be seen from table 6 that the value of C_{dl} increases from 0.23 to 0.3 mF/cm^2, for the samples having the Ti surface modification with amoxicillin. This behaviour is in agreement with the findings of our investigations [27].

Table 6

C_{dl} values calculated from CV diagrams for tested samples

Sample	C_{dl} (mF/cm^2)
Ti	0.23
Ti/AMX	0.30
NT_40V/AMX	0.81
NT_80V/AMX	0.84
RnT_40V/AMX	1.74
RnT_80V/AMX	1.58

The development of nanotubular structures on the titanium surface improve the surface's hydrophilicity, accelerating charge transfer at the interface and the production of electric double layers and thus the electrochemical capacitance of the porous structures of nanotubular samples which is significantly influenced by ion diffusion and charge transfer could be amplified.

The studied samples had high C_{dl} values, particularly the samples based reduced nanotubes (RnT_40V/AMX = 1.74 mF/cm^2 and RnT_80V/AMX = 1.58 mF/cm^2). This may indicate a more effective ion absorption/desorption process at the interface between the electrolyte solution and nanostructured surface.

4. *In vitro* amoxicillin release

First, the encapsulation efficiency was assessed using the difference between the initial concentrations (3g/L) and the final concentrations of amoxicillin remaining in the immersion solution, after extracting the sample. All nanostructured samples studied incorporated approximately the same amount of amoxicillin (60%), probably due to a better interaction between AMX and TiO_2 nanotubes (Fig.7).

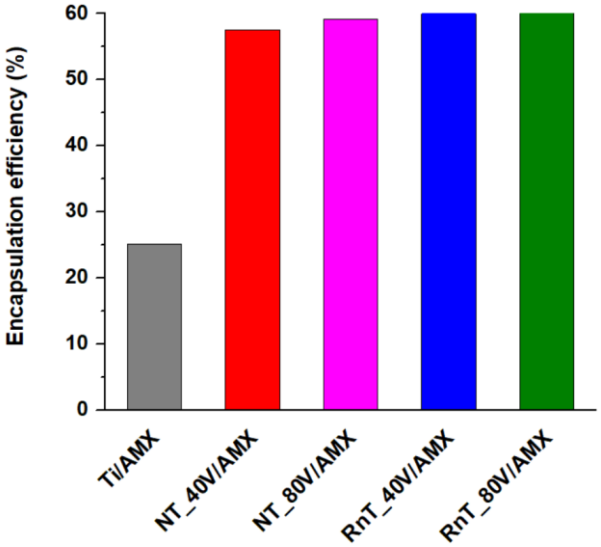

Fig. 7. The amoxicillin encapsulation efficiency.

The amoxicillin release curves of all the samples over 192 hours are seen in Fig. 8. There were not substantial changes in the first 120 hours between the NT_40V/AMX and NT_80V/AMX samples, the release of AMX being 40.32% and 39.38% respectively. In the case of the RnT_80V/AMX sample, was observed the slowest quantity of AMX released, at 26.82%. After 192 h, a drug release of 87.12% (Ti/AMX), 52.78% (NT_40V/AMX), 49.81% (NT_80V/AMX), 39.01% (RnT_40V/AMX) and 34.92% (RnT_80V/AMX) occurred.

Compared to the NT_40V and NT_80V substrates, the slower release may be achieved while using reduced nanotubes (RnT_40V and RnT_80V).

The distinct morphology of the TiO_2 nanotubes produced after anodizing can be used to explain this behaviour. The release is similar in the first hours because the antibiotic is released from the upper part of the nanotubes.

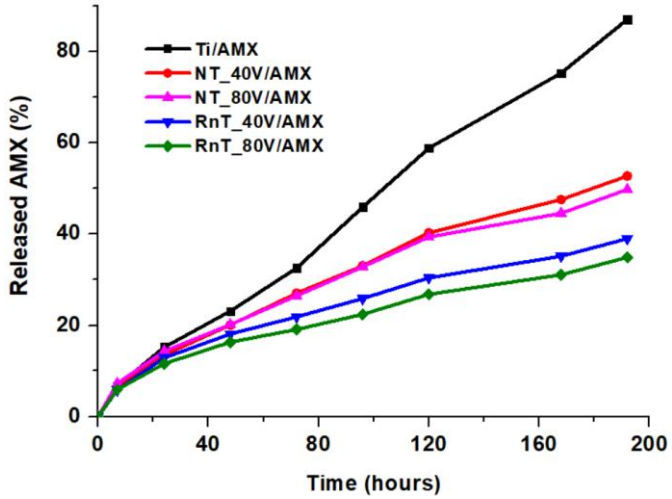

Fig. 8. AMX release in phosphate buffer

5. Conclusions

Ti surfaces were modified with TiO_2 nanotubular structures through an anodizing process, using different parameters. The selected nanostructured Ti samples were functionalized with an active compound, AMX. The active modified surfaces were characterized in terms of morphology, wettability, electrochemical stability and antibiotic release.

AMX integration in these nanostructures lead to a decrease of the contact angle values, being probably more beneficial for cell adhesion. All samples that were modified have a better corrosion resistance comparing with untreated titanium.

According to our investigations, the AMX may be fixed to the Ti nanostructured surface using either NT or RnT. In addition, RnT demonstrates improved performance in terms of amoxicillin delivery in time, this fact making these materials suitable for local drug delivery applications.

Acknowledgement

- ✓ The SEM analyses was funded by European Regional Development Fund through Competitiveness Operational Program 2014–2020, Priority axis 1, Project No. P_36_611, MySMIS code 107066

- ✓ This work has been funded by the European Social Fund from the Sectoral Operational Programme Human Capital 2014-2020, through the Financial Agreement with the title "Training of PhD students and postdoctoral

researchers in order to acquire applied research skills - SMART", Contract no. 13530/16.06.2022 - SMIS code: 153734.

R E F E R E N C E S

[1]. *S. Liu, X. Chen, M. Yu, J. Li, J. Liu, Z. Xie, et al.* Applications of Titanium Dioxide Nanostructure in Stomatology. Molecules. 2022;27(12):3881.

[2]. *J.J.E. Choi, J. Zwirner, R.S. Ramani, S. Ma, H.M. Hussaini, J.N. Waddell, et al.* Mechanical properties of human oral mucosa tissues are site dependent: A combined biomechanical, histological and ultrastructural approach. Clinical and experimental dental research. 2020;6(6):602-11.

[3]. *A.-S. Engel, H.T. Kranz, M. Schneider, J.P. Tietze, A. Piwowarcyk, T. Kuzius, et al.* Biofilm formation on different dental restorative materials in the oral cavity. BMC Oral Health. 2020;20(1):162.

[4]. *J.V. Califano, P.M. Preshaw.* 1 - Immunobiology of Infectious Disease. In: Hupp, J.R., Ferneini, E.M., editors. Head, Neck, and Orofacial Infections. St. Louis: Elsevier; 2016. p. 2-26.

[5]. *J. Mystkowska, K. Niemirowicz-Laskowska, D. Łysik, G. Tokajuk, J.R. Dąbrowski, R. Bucki.* The role of oral cavity biofilm on metallic biomaterial surface destruction–corrosion and friction aspects. International journal of molecular sciences. 2018;19(3):743.

[6]. *C. Cugini, N. Ramasubbu, V.K. Tsiagbe, D.H. Fine.* Dysbiosis From a Microbial and Host Perspective Relative to Oral Health and Disease. Frontiers in Microbiology. 2021;12.

[7]. *J. Park, A. Cimpean, A.B. Tesler, A. Mazare.* Anodic TiO(2) Nanotubes: Tailoring Osteoinduction via Drug Delivery. Nanomaterials (Basel, Switzerland). 2021;11(9).

[8]. *B. Chen, Y. Liang, Y. Song, Y. Liang, J. Jiao, H. Bai, et al.* Photothermal-Controlled Release of IL-4 in IL-4/PDA-Immobilized Black Titanium Dioxide (TiO(2)) Nanotubes Surface to Enhance Osseointegration: An In Vivo Study. Materials (Basel, Switzerland). 2022;15(17).

[9]. *S. Noreen, E. Wang, H. Feng, Z. Li.* Functionalization of TiO(2) for Better Performance as Orthopedic Implants. Materials (Basel, Switzerland). 2022;15(19).

[10]. *L. Yuan, X. Xu, X. Song, L. Hong, Z. Zhang, J. Ma, et al.* Effect of bone-shaped nanotube-hydrogel drug delivery system for enhanced osseointegration. Biomaterials Advances. 2022;137:212853.

[11]. *M. Benčina, A. Iglič, M. Mozetič, I. Junkar.* Crystallized TiO(2) Nanosurfaces in Biomedical Applications. Nanomaterials (Basel, Switzerland). 2020;10(6).

[12]. *R. Schenk.* The Corrosion Properties of Titanium and Titanium Alloys. 2001. p. 145-70.

[13]. *C. Jimenez-Marcos, J.C. Mirza-Rosca, M.S. Baltatu, P. Vizureanu.* Experimental Research on New Developed Titanium Alloys for Biomedical Applications. Bioengineering. 2022;9(11):686.

[14]. *Y. Huang, G. Zha, Q. Luo, J. Zhang, F. Zhang, X. Li, et al.* The construction of hierarchical structure on Ti substrate with superior osteogenic activity and intrinsic antibacterial capability. Scientific Reports. 2014;4(1):6172.

[15]. *E.P. Su, D.F. Justin, C.R. Pratt, V.K. Sarin, V.S. Nguyen, S. Oh, et al.* Effects of titanium nanotubes on the osseointegration, cell differentiation, mineralisation and antibacterial properties of orthopaedic implant surfaces. The bone & joint journal. 2018;100-b(1 Supple A):9-16.

[16]. *A. Mazare, J. Park, S. Simons, S. Mohajernia, I. Hwang, J.E. Yoo, et al.* Black TiO_2 nanotubes: Efficient electrodes for triggering electric field-induced stimulation of stem cell growth. Acta Biomaterialia. 2019;97:681-8.

[17]. *A. Roguska, M. Pisarek, A. Belcarz, L. Marcon, M. Holdynski, M. Andrzejczuk, et al.* Improvement of the bio-functional properties of TiO_2 nanotubes. Applied Surface Science. 2016;388.
[18]. *M. Wei, S. Li, W. Le.* Nanomaterials modulate stem cell differentiation: biological interaction and underlying mechanisms. Journal of Nanobiotechnology. 2017;15(1):75.
[19]. *M. Plodinec, I. Grčić, M.G. Willinger, A. Hammud, X. Huang, I. Panžić, et al.* Black TiO2 nanotube arrays decorated with Ag nanoparticles for enhanced visible-light photocatalytic oxidation of salicylic acid. Journal of Alloys and Compounds. 2019;776:883-96.
[20]. *T.S. Rajaraman, S.P. Parikh, V.G. Gandhi.* Black TiO_2: A review of its properties and conflicting trends. Chemical Engineering Journal. 2020;389:123918.
[21]. *K. Gulati, S. Makar, S. Chandrasekaran, D. Findlay, D. Losic.* Conversion of titania (TiO_2) into conductive titanium (Ti) nanotube arrays for combined drug-delivery and electrical stimulation therapy. J Mater Chem B. 2015;4.
[22]. *J. Park, A. Mazare, H. Schneider, K. von der Mark, M.J. Fischer, P. Schmuki.* Electric Field-Induced Osteogenic Differentiation on TiO2 Nanotubular Layer. Tissue engineering Part C, Methods. 2016;22(8):809-21.
[23]. *A.-M. Negrescu, V. Mitran, W. Draghicescu, S. Popescu, C. Pirvu, I. Ionascu, et al.* TiO_2 Nanotubes Functionalized with Icariin for an Attenuated In Vitro Immune Response and Improved In Vivo Osseointegration. Journal of Functional Biomaterials. 2022;13(2):43.
[24]. *M. Rozana, N.I. Soaid, T.W. Kian, G. Kawamura, A. Matsuda, Z. Lockman.* Photocatalytic performance of freestanding tetragonal zirconia nanotubes formed in H2O2/NH4F/ethylene glycol electrolyte by anodisation of zirconium. Nanotechnology. 2017;28(15):155604.
[25]. *X. Yan, L. Tian, X. Chen.* Black Titanium Dioxide (TiO_2) Nanomaterials. 2016. p. 1-26.
[26]. *N. ul Ain, I. Anis, F. Ahmed, M.R. Shah, S. Parveen, S. Faizi, et al*. Colorimetric detection of amoxicillin based on querecetagetin coated silver nanoparticles. Sensors and Actuators B: Chemical. 2018;265:617-24.
[27]. *A.G. Olaru, V. Butculescu, C. Dumitriu, N. Badea, S. Popescu, C. Ungureanu, et al.* Biopolymers as intermediate layers for amoxicillin grafting on antibacterial surface. Surfaces and Interfaces. 2022;33:102224.
[28]. *M. Ferrari, F. Cirisano, M.C. Morán.* Mammalian Cell Behavior on Hydrophobic Substrates: Influence of Surface Properties. Colloids and Interfaces. 2019;3(2):48.